

# Clinical and genetic analysis of ulnar-mammary syndrome caused by a novel *TBX3* mutation in a Chinese boy

Jianmei Yang<sup>1</sup>, Huimin Yu<sup>2</sup>, Yan Sun<sup>1</sup>, Chen Chen<sup>3</sup>, Guimei Li<sup>1,\*</sup>, Chao Xu<sup>2,\*</sup>

<sup>1</sup>Department of Paediatric Endocrinology, Shandong Provincial Hospital affiliated to Shandong First Medical University, Jinan, China;

<sup>2</sup>Department of Endocrinology, Shandong Provincial Hospital affiliated to Shandong First Medical University, Jinan, China;

<sup>3</sup>Endocrinology, SBMS, Faculty of Medicine, The University of Queensland, St Lucia, Australia.

**SUMMARY:** Ulnar-mammary syndrome (UMS) is caused by *TBX3* mutation and is a disorder characterized by altered limb, breast, tooth, hair, apocrine gland, and genital development. The clinical and genetic data of a 5.5<sup>th</sup> boy with UMS were carefully analyzed. Clinical biochemical data, pituitary MRI, and whole exome gene detection were analyzed. The impact of the mutation and stability of *TBX3* on the mRNA structure was analyzed by the M-fold program. Three-dimensional protein structures were calculated and analyzed. The patient presented with a hypoplastic left fifth finger, an absence of interphalangeal creases, a large space between the fourth and fifth fingers, no bending ability of the fifth finger, absent nipples, high palates, a flat nasal bridge, a micropenis, micro-testes, short stature and reduced axillary sweating. Pituitary magnetic resonance imaging (MRI) revealed pituitary gland hypoplasia with a thin pituitary stalk and loss of a strong signal in the posterior pituitary. A novel variant (c.1142\_1146) in the *TBX3* gene was detected in the proband and further verified by DNA sequencing. M-fold results revealed that the variant altered the mRNA structure and stability of the *TBX3* gene. Clinical, genetic, and biochemical studies confirmed that the congenital normal idiopathic hypogonadotropic hypogonadism was associated with pituitary hypoplasia. After half a year of treatment with human chorionic gonadotropin (HCG), the micropenis was significantly improved. After 3.5 years of treatment with recombinant human growth hormone, the body height was largely improved. One novel variant of the *TBX3* gene was confirmed in an UMS patient, which enriched the spectrum of *TBX3* genotypes.

**Keywords:** ulnar-mammary syndrome, *TBX3*, micropenis, HCG, hGH

## 1. Introduction

Ulnar-mammary syndrome (UMS; MIM #181450), an autosomal-dominant disorder, is caused by mutations in *TBX3* (1). Despite the fact that such ulnar deficiencies may scarcely occur in 1 out of 25,000 births (2), the exact incidence of UMS is still unknown. Asymmetrical ulnar ray defects with shortening of the fifth digit or complete absence of the ulna radius, combined with hand defects, hypoplasia of the breast (areola and nipple), aphobia, subfertility with gonad deficiency, genital deviation, short stature, dental anomalies, cardiac defects, and obesity were observed.

The disorder displays obvious interfamilial and intrafamilial changes in phenotype. To date, twenty-two *TBX3* pathogenic variants with considerable insertions or deletions have been reported (1,3-11). UMS has some overlapping features with certain other syndromes. The main syndromes that overlap with UMS include the allelic disorders of acro-dermato-ungual-lacrima-tooth

syndrome (MIM #103285) (12) and limb-mammary syndrome (MIM #603543) (13); both are caused by *TP63* gene mutations. Other overlaps exist with scalp-ear-nipple syndrome (MIM #181270), which is caused by *KCTD1* gene mutations (14). Genetic examination of UMS is therefore crucial for obtaining an accurate diagnosis.

We have carefully reviewed the literature using PubMed and WANFANG MED ONLINE. In this study, a novel variant in the *TBX3* gene was identified in a boy, which was the 4<sup>th</sup> reported case in China, with three previously reported cases (15-17). The deteriorating property of such mutation was verified by bioinformatic analysis. A follow-up study was completed to determine the prognosis of the patient after hormonal treatment. UMS clearly showed abundant variability in its mutational heterogeneity, phenotypic presentation, and ethnic diversity, as evidenced here in the report.

## 2. Patient and Methods

### 2.1. Ethical approval

The Institutional Human Ethics Review Board at Shandong Provincial Hospital affiliated to Shandong First Medical University approved this study (LCYJ:NO. 2019-147). The legal guardians of the participant were given written information to obtain signed consent to participate in the study. This study conforms to the provisions of the Declaration of Helsinki.

### 2.2. Patient

In 2021, a 5.5-year-old male patient visited the outpatient department of Paediatric Endocrinology, Shandong Provincial Hospital, for micropenis and retarded body growth. The parents of this patient were physically healthy and nonconsanguineous. The clinical evaluation, baseline and dynamic hormonal levels, and genetic analyses were obtained from the patient with signed consent from the parents.

### 2.3. Clinical observations

The following hormones were measured in the serum samples: follicle stimulating hormone (FSH), luteinizing hormone (LH), progesterone, estrogen, testosterone, adrenocorticotrophic hormone (ACTH), thyroid-stimulating hormone (TSH), free triiodothyronine (FT3), free thyroxine (FT4), and insulin-like growth factor-1 (IGF-1). Gonadotrophin-releasing hormone (GnRH) stimulation tests (those involving intravenous injection of GnRH and LH and FSH at baseline and +30', +60', +90' after GnRH injection), and growth hormone releasing hormone (GHRH) stimulation tests (those involving intravenous injection of GHRH and blood sample collection for GH determination at baseline and +30', +60', +90', +120', +150' after GHRH injection) were conducted with standard procedures. All hormones were measured by chemiluminescent methods (Roche, Basel, Switzerland) following the manufacturer's instructions. Blood electrolyte levels, routine blood tests, and qualitative urine calcium levels were measured in the hospital laboratory. Additionally, magnetic resonance imaging (MRI), bone age, and funduscopic examination were also carried out in the hospital.

### 2.4. Genome sequencing

Peripheral venous blood (3-5 mL) was collected from the proband and his parents. Peripheral blood DNA was sequenced using whole exome sequencing (WES). The exons from patient genomic DNA were fragmented, ligated, amplified, and purified following the manufacturer's protocol, and then examined with the SeqCap EZ Med Exome Enrichment Kit (Roche NimbleGen) according to the manufacturer's protocol. The exons and flanking regions of all known genes

were captured. After postcapture amplification and purification, the Illumina HiSeq system was used to construct the DNA library.

The sequence data were aligned to the human genome reference 19 (hg19) by NextGene V2.3.4 to secure good coverage and depth of the mean reading of the target regions. Conserved nucleotide bases and amino acids, frequency of the normal populations (1000 Genomes Project, ExAC, dbSNP DNA and locus specific databases), predictions of the biological functions, and data from The Human Gene Mutation Database (HGMD) and Clinvar and Online Mendelian Inheritance in Man (OMIM), were obtained using NextGene V2.3.4. Variants were screened according to the published rules. Pathogenicity variants were interpreted by the American College of Medical Genetics (ACMG) guidelines for the interpretation of sequence variants published in 2015 using the Human Genome Variation Society (HGVS) nomenclature.

Sanger sequencing was used to verify the variants in the proband revealed by WES, and to test the cosegregation of variants in the family. Genome sequencing was completed in collaboration with Berry Genomics Co.

### 2.5. Bioinformatic analysis

Bioinformatics tools are widely used for predicting and understanding the effects of genetic variants on the structure, stability and function of proteins and mRNA stability (18). Therefore, in this study, the disease-causing potential of the genetic variants was extensively analyzed using the silico methods.

To determine the changes in RNA thermodynamic stability caused by mutations, the changes before and after mutations were compared. The secondary structure of RNA influences the expression of genes by changing the stability of RNA or transcript, and the efficiency of translation. The mutation may alter the sequence of the mRNA and the secondary structure of RNA. Changes in the RNA structure or thermodynamic stability may affect the rate of mRNA translation into proteins. In this study, variations in the *TBX3* mRNA secondary structure and stability were predicted by the M-fold server (<http://unafold.rna.albany.edu/?q=mfold/RNA-Folding-Form>). The input sequences consisted of two different lengths of mRNA fragments, i.e 75 bases and 150 bases with the variant of interest centered in the middle of the mRNA fragments. Most of the predicted stable structures with minimum  $\delta G$  values were chosen for further calculation of the minimum free energy ( $\delta\delta G$ ) of the mutant mRNA and wild-type mRNA ( $\delta\delta G = \delta G_{\text{mutant}} - \delta G_{\text{wild-type}}$ ). The greater the positive  $\delta\delta G$  value, the lower the stability of the mutated mRNA relative to the wild-type mRNA. Our previous inputs consisted of short-length RNA fragments, as the complexity of potential structures increases exponentially with longer sequences, leading to

a decrease in prediction accuracy (18).

We demonstrated the spatial structure of the *TBX3* protein and the affected protein regions after generation of frameshift mutations. Prediction of three-dimensional protein structures based on the three-dimensional structure of mutant *TBX3* was achieved using I-TASSER software (19) (<https://zhanglab.ccmb.med.umich.edu/I-TASSER/>). The PyMOL Viewer software was used to visualize the effects of altered residues on the protein structure models.

### 3. Results and Discussion

UMS was first reported by McKusick in 1975 (20). A variety of abnormalities have been reported in addition to limb and apocrine defects (21) over the last few years. Various postaxial limb defects exist, such as hypoplastic distal phalanges in digit V or absent digits III-V with radial shortening of the ulnae.

When the condition is more severe, the hand, ulna, radius, and humerus are all absent. UMS patients may also exhibit dorsal hypoplasia/aplasia of the breast, absence of axillary hair, reduced or absent perspiration, short stature, obesity, delayed puberty, dental abnormalities, hypopigmentation of the nipples and areola, genital hypoplasia, cardiac defects, anatomical pituitary anomalies and scoliosis (8,15,16,22,23).

In this report, the patient had normal mental and nutritional status and a height of 107.8 cm (P3-10). He had a hypoplastic left fifth finger with no interphalangeal creases, and a wide space between the fourth and fifth fingers, and the fifth finger could not bend. He also had absent nipples, high palates, micropenis, flat nasal bridge, irregularly arranged teeth, a micropenis (1.5 cm × 1 cm), micro-testis (< 1 mL), and reduced axillary sweating (Figure 1). His parents had no similar symptoms.

Evaluation of hormone levels showed reduced testosterone (TO) (< 0.03 ng/mL), LH (< 0.1 mIU/mL) and FSH (0.76 mIU/mL) levels. The following parameters were used: normal IGF-1 (55 ng/mL, reference ranges: 45-305 ng/mL); TSH (2.14 µIU/mL, reference ranges: 0.7-4.17 µIU/mL); free T4 (15.95 pmol/L, reference ranges: 11.45-17.63 pmol/L); and prolactin (12.87 ng/mL, reference ranges: 4.04-15.2 ng/mL). After intramuscular injection of 1,000 U human chorionic gonadotropin (HCG) every week for approximately half a year, the level of TO (2.20 ng/ml) was increased, that of FSH (0.17 mIU/ml) decreased, and that of LH did not change.

MRI of the pituitary of this 5.5-year-old patient (taken on 2021-06-06) revealed that the upper edge of the pituitary was concave, the height of the adenohypophysis was approximately 3 mm, and the picture showed a thin pituitary stalk and a loss of high signal in the posterior pituitary, suggesting a clear pituitary gland hypoplasia.

A novel variant in the *TBX3* gene was observed by WES in the proband and confirmed by Sanger

sequencing (15). A heterozygous *TBX3* variant NM\_005996.4:exon6:c.1142\_1146dup(p.P383 the Rfs\*231) was identified (Figure 2). The score was PVS1\_Strong+PM2+PM6, which was regarded as a pathogenic mutation according to ACMG Guidelines (24). Sanger sequencing confirmed that this new variant was not transmitted from the parents of this patient.

*TBX3*, located on chromosome 12q24.21, is an ancient and evolutionarily conserved T-box transcription factor. It plays an important role in the control of developmental signal systems (25) involved in critical structure formation of organs, such as the mammary glands, heart, lungs and limbs (26). All organs are developed on the highly conserved T-box DNA-binding domain, which is generally encoded by exons 1-3 and a part of exon 4 (27). The T-box is expressed in specific tissues of the developing embryo and is required for tissue differentiation. There is a close relationship between *TBX3* and *TBX5* on chromosome 12. For the differentiation of radial limbs, *TBX5* expression is essential, while *TBX3* controls ulnar limb development. A mutation in *TBX5* causes Holt-Oram syndrome, which is characterized by radial longitudinal deficiency and cardiac defects (28). UMS is believed to be mainly caused by *TBX3* haploinsufficiency. Patients with UMS are predicted to have mutations that disrupt the transcriptional regulation or render the proteins susceptible to degradation by nonsense mediated decay. To date, *TBX3* mutations and UMS clinical manifestations have little genotype-phenotype correlation (3,5).

This patient had a classical high palate, micropenis, flat nasal bridge, broad hands, and multiple pituitary hormone deficiencies. The mutation lies within exon 6 of the *TBX3* gene. As a result, amino acid 383 was changed from proline to arginine, which was terminated after amino acid 231, and may still retain some function or may be eliminated by nonsense-mediated RNA decay. In addition to this patient, other individuals with UMS with mutations downstream of the T domains were identified. Meneghini *et al.* (7) hypothesized that the presence of an intact T-box domain was most likely allowed for residual DNA-binding activity, leading to a milder clinical phenotype. However, other researchers (3,8) have clearly shown a correlation between classical UMS phenotypes and mutations preserving this T-box domain. Recently, the ability of the C-terminal domain of *TBX3* to interact with mRNAs and to regulate alternative splicing has been reported. Mutations found in UMS patients with truncated *TBX3* 5' of the T-box domain were shown to dominantly interfere with the function in inhibiting splicing (29). *TBX3* mutations included two categories: those located within the location 5-prime of the T-box, or within the T-box, and mutations located 3-prime of the T-box. In this study, the mutation was located at the 3' end, downstream of the T-box domain.

No other variants in *TBX3* were observed to modify

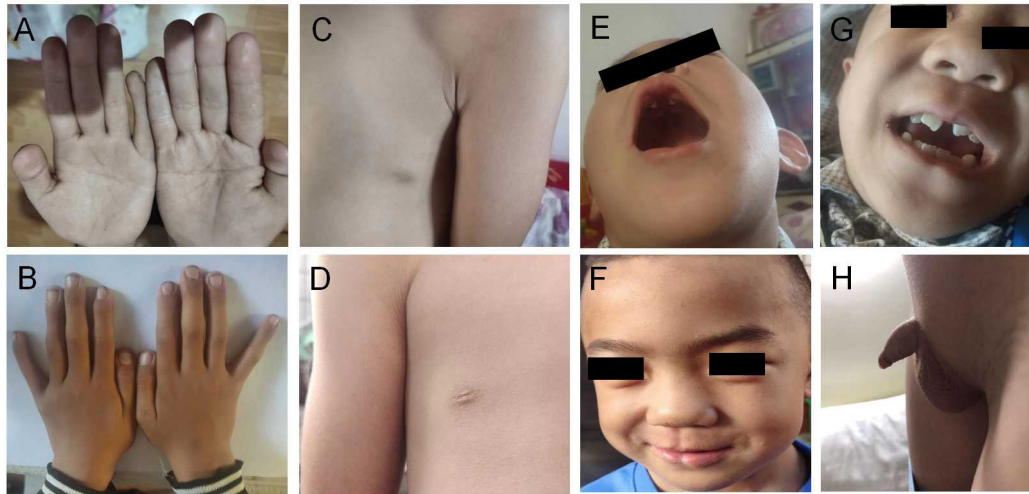


**Figure 1. The clinical features of patient.** (A, B) Hypoplastic left fifth fingers with absent interphalangeal creases, wide space between the fourth and fifth fingers, and the fifth finger cannot be bent. (C, D) Absent nipples. (E) High palates. (F) Flat nasal bridge. (G) Irregularly arranged teeth, and (H) Micropenis.

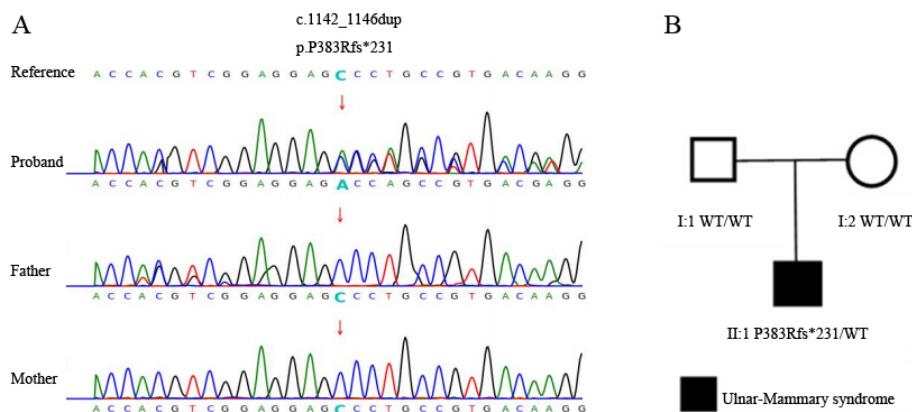


**Figure 2. The genetic analysis.** (A) *TBX3* gene mutation analysis of the patient (GenBank accession number: NM\_005996.4). (B) The pedigree of this family.

the phenotype, and the factors causing phenotypic variability in this patient could not be identified. The phenotypic variability found in UMS families may be caused by the different degree of changes in *TBX3* function during embryonic development (30). It is also possible that other genetic variants may affect a similar function, causing UMS during development, which may contribute to variations in severity and affected organs.

The effect of c.1142\_1146dup on mRNA structure and stability was evaluated by the M-fold server to predict substantial alterations in mutated mRNAs compared with the wild-type mRNAs. This mutation changed the mRNA sequence and the secondary structure of the transcript. After mutation, the original multiloop was changed, and a new hairpin loop was formed. The overall and partial structures of the wild-type and mutant mRNAs are shown in Figure 3. The greater the optimal

energy is, the less stable the RNA. The variant increased the optimal energy and decreased the mRNA stability (Figure 4A, B). The three-dimensional protein structure model of the P383Rfs\*231 mutant *TBX3* protein (green showing the affected area) is shown in Figure 4C.

This patient was followed up closely since his diagnosis. During the follow-up period, HCG treatment was given for 6 months (NaCl 1ml + HCG 1000 iu im qw). The micropenis was improved from 1.5 × 1 cm to 4 × 3 cm. After 3.5 years of treatment with recombinant human growth hormone (rhGH 0.15 u/kg ih qn), his height improved from 107.8 cm (P3-10) (5.5 years) to 135.2 cm (Near P50) (9 years). Additionally, thyroid hormones, blood electrolytes, IGF-1, ACTH, routine blood test, and qualitative urine calcium were monitored regularly and maintained within the normal range.

All the allelic variants reported in the literature and

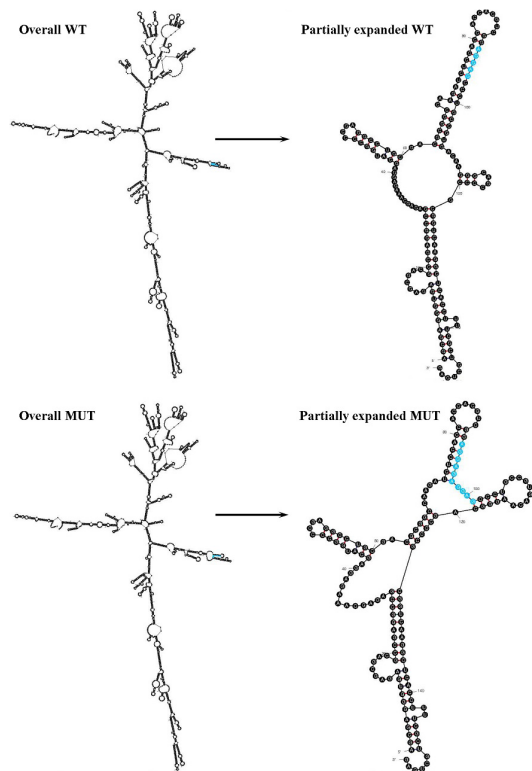


**Figure 3. The analysis of the Mfold RNA secondary structure.** Blue indicates the wild/mutated bases. The overall wild-type (WT) and mutant-type (MUT), and partially expanded WT and MUT structures are placed up and down for comparison, respectively.

HGMD were reviewed to better understand the genotype-phenotype correlations in *TBX3*-related disorders (Supplemental Table S1, <https://www.irdrjournal.com/supplementaldata/250>). To date, 38 mutations in *TBX3* have been identified and most of these mutations are missense or nonsense mutations (17/38 or 44.74%), followed by deletions, insertions, and splicing mutations. However, *TBX3* mutation locations have not been related to any clinical disorders yet.

In conclusion, the other three previously reported cases in China (15-17) are mainly case reports with literature review, but do not include any bioinformatic analysis. This current work is the first UMS case with bioinformatic analysis in China. Further evidence is provided to demonstrate the variability in mutational heterogeneity, phenotypic expression, and ethnic diversity involved in this specific phenotype of UMS. In addition, UMS may be associated with dwarfism with special facial characteristics and dysplasia of the external genitalia, sweat glands, and mammary glands. *TBX3* is a pathogenic gene of UMS.

**Acknowledgements**

We are grateful to the patient and parents for their contribution to the study. The authors would also like to thank the Xiaotian Su and Berry Genomics Co. for the

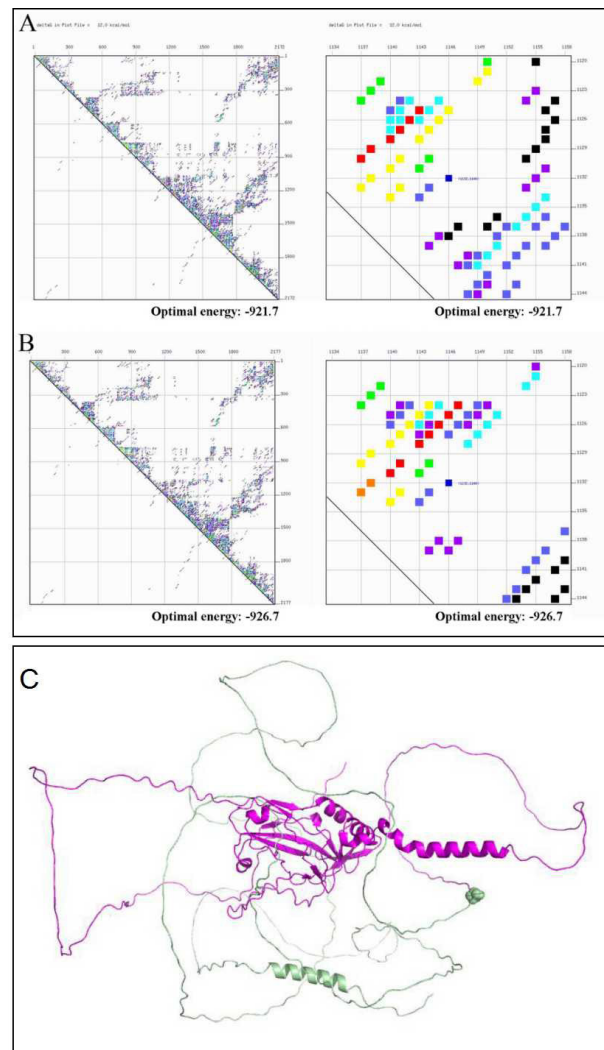


**Figure 4. The analysis of the wild-type and mutant-type mRNA stability, and 3-D modelling of wild-type and P383Rfs\*231 mutant *TBX3* protein.** The differences in the alignment of wild-type (purple) and mutant (green) *TBX3* protein in 3-D modelling.

technical support to this study.

**Funding:** This work was supported by National Natural Science Foundation of China (82100920), Natural Science Foundation of Shandong Province (CN) (ZR2024MH184, ZR2020MH107 and ZR2020MH102), Young and Middle-aged Innovative Talents Project of Shandong Provincial Hospital.

**Conflict of Interest:** The authors have no conflicts of interest to disclose.

**References**

1. Klopocki E, Neumann LM, Tönnies H, Ropers HH, Mundlos S, Ullmann R. Ulnar-mammary syndrome with dysmorphic facies and mental retardation caused by a novel 1.28 Mb deletion encompassing the *TBX3* gene. *Eur J Hum Genet.* 2006; 14:1274-1279.
2. Koskimies E, Lindfors N, Gissler M, Peltonen J,

- Nietosvaara Y. Congenital upper limb deficiencies and associated malformations in Finland: A population-based study. *J Hand Surg Am.* 2011; 36:1058-1065.
3. Bamshad M, Le T, Watkins WS, *et al.* The spectrum of mutations in *TBX3*: Genotype/Phenotype relationship in ulnar-mammary syndrome. *Am J Hum Genet.* 1999; 64:1550-1562.
  4. Sasaki G, Ogata T, Ishii T, Hasegawa T, Sato S, Matsuo N. Novel mutation of *TBX3* in a Japanese family with ulnar-mammary syndrome: Implication for impaired sex development. *Am J Med Genet.* 2002; 110:365-369.
  5. Wollnik B, Kayserili H, Uyguner O, Tükel T, Yuksel-Apak M. Haploinsufficiency of *TBX3* causes ulnar-mammary syndrome in a large Turkish family. *Ann Genet.* 2002; 45:213-217.
  6. Borozdin W, Bravo-Ferrer Acosta AM, Seemanova E, Leipoldt M, Bamshad MJ, Unger S, Kohlhase J. Contiguous hemizygous deletion of *TBX5*, *TBX3*, and *RBM19* resulting in a combined phenotype of Holt-Oram and ulnar-mammary syndromes. *Am J Med Genet A.* 2006; 140a:1880-1886.
  7. Meneghini V, Odent S, Platonova N, Egeo A, Merlo GR. Novel *TBX3* mutation data in families with ulnar-mammary syndrome indicate a genotype-phenotype relationship: Mutations that do not disrupt the T-domain are associated with less severe limb defects. *Eur J Med Genet.* 2006; 49:151-158.
  8. Linden H, Williams R, King J, Blair E, Kini U. Ulnar Mammary syndrome and *TBX3*: Expanding the phenotype. *Am J Med Genet A.* 2009; 149A:2809-2812.
  9. Joss S, Kini U, Fisher R, Mundlos S, Prescott K, Newbury-Ecob R, Tolmie J. The face of Ulnar Mammary syndrome? *Eur J Med Genet.* 2011; 54:301-305.
  10. Alby C, Bessieres B, Bieth E, Attie-Bitach T, Fermont L, Citony I, Razavi F, Vekemans M, Escande F, Manouvrier S, Malan V, Amiel J. Contiguous gene deletion of *TBX5* and *TBX3* leads to a variable phenotype with combined features of Holt-Oram and ulnar-mammary syndromes. *Am J Med Genet A.* 2013; 161A:1797-1802.
  11. Bogarapu S, Bleyl SB, Calhoun A, Viskochil D, Saarel EV, Everitt MD, Frank DU. Phenotype of a patient with contiguous deletion of *TBX5* and *TBX3*: Expanding the disease spectrum. *Am J Med Genet A.* 2014; 164A:1304-1309.
  12. Slavotinek AM, Tanaka J, Winder A, Vargervik K, Haggstrom A, Bamshad M. Acro-dermato-ungual-lacrimal-tooth (ADULT) syndrome: Report of a child with phenotypic overlap with ulnar-mammary syndrome and a new mutation in *TP63*. *Am J Med Genet A.* 2005; 138A:146-149.
  13. van Bokhoven H, Jung M, Smits AP, van Beersum S, Rüschenhoff F, van Steensel M, Veenstra M, Tuerlings JH, Mariman EC, Brunner HG, Wienker TF, Reis A, Ropers HH, Hamel BC. Limb mammary syndrome: A new genetic disorder with mammary hypoplasia, ectrodactyly, and other Hand/Foot anomalies maps to human chromosome 3q27. *Am J Hum Genet.* 1999; 64:538-546.
  14. Marneros AG, Beck AE, Turner EH, *et al.* Mutations in *KCTD1* cause scalp-ear-nipple syndrome. *Am J Hum Genet.* 2013; 92:621-626.
  15. Zhang X, Chen L, Li L, An J, He Q, Zhang X, Lu W, Xiao Y, Dong Z. Literature review, report, and analysis of genotype and clinical phenotype of a rare case of ulnar-mammary syndrome. *Front Pediatr.* 2023; 11:1052931. (in Chinese)
  16. Peng N, Guo M, Jiang T. Ulnar-Mammary syndrome with *TBX3* gene mutation in a Chinese family: A case report and literature review. *Zhong Nan Da Xue Xue Bao Yi Xue Ban.* 2022; 47:1769-1774. (in Chinese)
  17. Wang XY, Chen XL, Wu HY, Xie RR, Wang FY, Chen T, Sun H, Zhang D. Clinical and genetic analysis of Ulnar-Mammary syndrome caused by *TBX3* de novo mutation in a boy and literature review. *Chinese Journal of Endocrinology and Metabolism.* 2020; 36:593-597. (in Chinese)
  18. Yadav ML, Jain D, Neelabh, Agrawal D, Kumar A, Mohapatra B. A gain-of-function mutation in *CITED2* is associated with congenital heart disease. *Mutat Res.* 2021; 822:111741.
  19. Yang J, Yan R, Roy A, Xu D, Poisson J, Zhang Y. The I-TASSER Suite: Protein structure and function prediction. *Nat Methods.* 2015; 12:7-8.
  20. Schinzel A. Ulnar-mammary syndrome. *J Med Genet.* 1987; 24:778-781.
  21. Bamshad M, Lin RC, Law DJ, Watkins WC, Krakowiak PA, Moore ME, Franceschini P, Lala R, Holmes LB, Gebuhr TC, Bruneau BG, Schinzel A, Seidman JG, Seidman CE, Jorde LB. Mutations in human *TBX3* alter limb, apocrine and genital development in ulnar-mammary syndrome. *Nat Genet.* 1997; 16:311-315.
  22. Tung ML, Chandra B, Kotlarek J, Melo M, Phillippi E, Justice CM, Musolf A, Boyadijev SA, Romitti PA, Darbro B, El-Shanti H. *TBX3* and *EFNA4* Variant in a Family with Ulnar-Mammary Syndrome and Sagittal Craniosynostosis. *Genes (Basel).* 2022; 13:1649.
  23. Al-Qattan MM, Maddirevula S, Alkuraya FS. A de novo *TBX3* mutation presenting as dorsalization of the little fingers: A forme fruste phenotype of ulnar-mammary syndrome. *Eur J Med Genet.* 2020; 63:103615.
  24. Richards S, Aziz N, Bale S, Bick D, Das S, Gastier-Foster J, Grody WW, Hegde M, Lyon E, Spector E, Voelkerding K, Rehms HL. Standards and guidelines for the interpretation of sequence variants: A joint consensus recommendation of the American College of Medical Genetics and Genomics and the Association for Molecular Pathology. *Genet Med.* 2015; 17:405-424.
  25. Papaioannou VE. T-box genes in development: From hydra to humans. *Int Rev Cytol.* 2001; 207:1-70.
  26. Khan SF, Damerell V, Omar R, Du Toit M, Khan M, Maranyane HM, Mlaza M, Bleloch J, Bellis C, Sahn BDB, Peres J, ArulJothi KN, Prince S. The roles and regulation of *TBX3* in development and disease. *Gene.* 2020; 726:144223.
  27. Wilson V, Conlon FL. The T-box family. *Genome Biol.* 2002; 3:REVIEWS3008.
  28. Naiche LA, Harrelson Z, Kelly RG, Papaioannou VE. T-box genes in vertebrate development. *Annu Rev Genet.* 2005; 39:219-239.
  29. Kumar PP, Franklin S, Emechebe U, Hu H, Moore B, Lehman C, Yandell M, Moon AM. *TBX3* regulates splicing *in vivo*: A novel molecular mechanism for Ulnar-mammary syndrome. *PLoS Genet.* 2014; 10:e1004247.
  30. Frank DU, Carter KL, Thomas KR, Burr RM, Bakker ML, Coetzee WA, Tristani-Firouzi M, Bamshad MJ, Christoffels VM, Moon AM. Lethal arrhythmias in *Tbx3*-deficient mice reveal extreme dosage sensitivity of cardiac conduction system function and homeostasis. *Proc Natl Acad Sci U S A.* 2012; 109:E154-E163.

Received December 29, 2024; Revised February 25, 2025;

Accepted March 24, 2025.

*\*Address correspondence to:*

Chao Xu, Department of Endocrinology, Shandong Provincial Hospital affiliated to Shandong First Medical University, 324 Jingwu Road, Jinan 250021, China.  
E-mail: doctorxuchao@163.com

Guimei Li, Department of Paediatric Endocrinology, Shandong Provincial Hospital affiliated to Shandong First Medical University, 9677 Jingshi Road, Jinan 250021, China.  
E-mail: liguimei2013@126.com

Released online in J-STAGE as advance publication April 2, 2025.